engineering proceedings

MDPI

Proceeding Paper

Simulation of Low-Frequency Sonophoretic Piezoelectric Transducer Applied over Human Skin †

Sehreen Moorat [1,*], Ahsan Ahmed Ursani [2], Aftab Memon [3], Nashrul Fazli Mohd Nasir [4] and Bhawani S. Chowdhry [5]

[1] Institite of Biomedical Engineering and Technology, Liaquat University of Medical Health and Sciences, Jamshoro 71000, Pakistan
[2] Department of Biomedical Engineering, Mehran University of Engineering & Technology, Jamshoro 71000, Pakistan; ahsan.ursani@faculty.muet.edu.pk
[3] Department of Telecommunication Engineering, Mehran University of Engineering & Technology, Jamshoro 71000, Pakistan; aftab.memon@faculty.muet.edu.pk
[4] Faculty of Electronic Engineering Technology, Universiti Malaysia Perlis, Arau 02600, Malaysia; nashrul@unimap.edu.my
[5] Faculty of Electrical, Electronics, & Computer Engineering, Mehran University of Engineering & Technology, Jamshoro 71000, Pakistan; c.bhawani@ieee.org
* Correspondence: sehreen.moorat@lumhs.edu.pk
† Presented at the 2nd International Conference on Emerging Trends in Electronic and Telecommunication Engineering, Karachi, Pakistan, 15–16 March 2023.

Abstract: Sonophoresis is the process that involves the passage of drug molecules through the skin under ultrasonic stimulation. Drugs with a molecular weight greater than 500 daltons require some kind of stimulus to catalyze their penetration into the skin. Low-frequency sonophoresis, i.e., applying low-frequency (20–100 kHz) ultrasonic waves, is one of the active methods of stimulation used in transdermal drug delivery. The aim of this research is to explore the possibility of achieving high enough acoustic pressures inside human skin using a single-element piezoelectric transducer required to realize the transdermal delivery of drugs with a high molecular weight. Therefore, this paper presents a design and simulation of a single-element transducer to find voltage versus sound pressure levels (SPLs), as well as frequency response curves for low-frequency sonophoresis on human skin. A piezoelectric transducer composed of PZT-5H placed over human skin was simulated by combining the pressure acoustic module, solid mechanics, and electrostatic modules of the simulation tool. The presented simulation applies sinusoidal excitation to a PZT-5H-based transducer. The peak voltage and the frequency of the input are varied to study the resulting variations in acoustic pressure and SPL inside the human skin. Measurements of acoustic pressure are taken 0.1 mm deep into the human skin. The peak acoustic pressure increases linearly from 0.072 Pa to 0.72 Pa as the peak applied voltage increases from 1 mV to 10 mV. The peak acoustic pressure increases exponentially from 0.2 mPa to 5 mPa as the frequency varies from 20 kHz to 100 kHz for a constant peak voltage of 1 mV. The SPL achieved at 880 kHz is 186 dB, which is suitable for drug delivery in some areas of medicine, such as ophthalmology.

Keywords: drug delivery; transdermal; sonophoresis; piezoelectric transducer; simulation; COMSOL

Citation: Moorat, S.; Ursani, A.A.; Memon, A.; Nasir, N.F.M.; Chowdhry, B.S. Simulation of Low-Frequency Sonophoretic Piezoelectric Transducer Applied over Human Skin. *Eng. Proc.* **2023**, *32*, 14. https://doi.org/10.3390/engproc2023032014

Academic Editors: Muhammad Faizan Shirazi, Saba Javed, Sundus Ali and Muhammad Imran Aslam

Published: 25 April 2023

1. Introduction

Sonophoresis is a kind of stimulation that uses ultrasonic waves for the enhancement of movement of drug molecules through the skin. It uses low-frequency ultrasonic waves (20–100 kHz) to promote transdermal absorption [1] of a drug. It is widely used to increase the permeability of skin by altering the internal structure of the epidermis. The mechanisms of disrupting the epidermis barrier underlying sonophoresis include thermal effects and cavitation. The latter causes formation of cavities due to pre-existing gas bubbles in a lipid

bilayer. The repeated expansion and contraction opens a channel of pores, which the drug penetrates through Ref. [2]. The maximum pressure required to produce cavitation inside the skin is 0.2 MPa.

Drug delivery systems (DDSs) are technologies by which controlled release of therapeutic drugs can be delivered to a targeted area [3]. Different routes are used to administer drugs into the human body. The examples include ocular, nasal, anal, buccal, oral, sublingual, pulmonary, and transdermal. Among different types of DDSs, transdermal drug delivery has many advantages over others, including uniform drug plasma concentration, elimination of hepatic first pass, and avoiding degradation in the gastrointestinal tract [4]. Transdermal drug delivery is achieved through either active or passive methods. Drugs with a molecular weight of less than 500 daltons [5], i.e., nitroglycerin (227.0 daltons), scopolamine (303.3 daltons), fentanyl (336.4 daltons), nicotine (162.23 daltons), and lidocaine (234.32 daltons) [6], can easily penetrate without requiring any stimulus. Meanwhile, the top-most layer of human skin, i.e., the epidermis, behaves like a barrier to the passage of the drugs with large molecular weights. Therefore, drugs with a molecular weight greater than 500 daltons, such as insulin (5734 daltons), tetanus toxoid (100 kDa), and bovine serum albumin (66,430.3 daltons) [7], require active methods employing a stimulus to disrupt the epidermis. The active methods of stimulation include iontophoresis [8], electroporation [9], photomechanical waves or lasers [10], and sonophoresis [11]. Besides transdermal drug delivery, sonophoresis is found in various other medical applications too, i.e., it is used to promote drug release in the digestive tract through an endoscope [12], dental applications [13], body contouring [14], wound healing [15], arthritis [16], etc.

Permeability of human skin depends on its thickness, which is different at different sites of the human body [13], as well as in race, age group, and gender [14]. For reasons of practical convenience, we considered the site of the volar forearm where the average thickness of the epidermis is 0.1 mm [15], and in this simulation, the acoustic pressure is measured at the lower end of epidermis as shown in Figure 1.

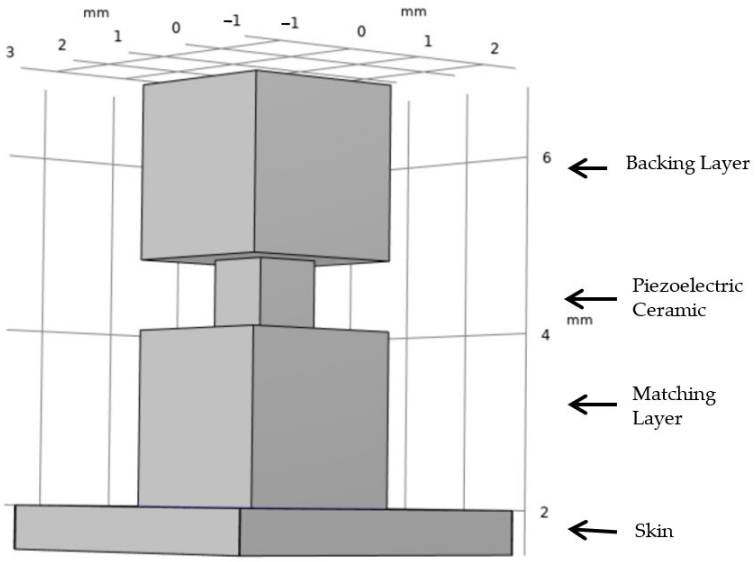

Figure 1. Geometry of single-element piezoelectric transducer.

Piezoelectric material has the capability to convert electrical energy into mechanical energy and vice versa. These materials generate electric charge upon applying stress (direct effect) and exhibit mechanical deformation upon applying an electric field (converse effect) [17]. The types of piezoelectric materials include ceramics, such as lead zirconate titanate, barium titanate, lithium niobate, and composites comprising polymers and ceramics. Among the available types, in this work, lead zirconate titanate (PZT-5H) is selected due to its exceptional tailorable properties as a medical transducer. PZT is used in various other applications, such as in microphones, loudspeakers, ultrasound transducers, actuators, sensors, etc.

Hence, the aim of this paper is to simulate a compact single-element piezoelectric transducer which operates at low frequency and low electrical power. However, the results of a single piezoelectric element are presented in terms of acoustic pressure and SPL inside the human skin against varying voltage and varying excitation frequency. However, obtaining results on drug delivery is out of the scope of this paper.

2. Literature Review

Besides transdermal drug delivery, many authors have reported the use of sonophoresis in non-medical applications, such as removing algae bloom from river water [9], to observe bacterial growth in biofilms [10], in biotechnological processes [11], etc.

As far as transdermal delivery of drugs is concerned, many researchers have experimented with various active and passive techniques for drugs of varying molecular weight. Chaulagain et al. [18] experimented with active and passive methods for the transport of drug delivery of protein and peptides. Active methods (sonophoresis, microneedle, iontophoresis) are faster compared to passive methods (prodrugs, nanocarriers) because they can easily disrupt the skin by applying additional pressure. By combining active and passive methods, such as microneedle with liposomes [19], the flux of passing insulin in the body increased 713.3 fold when compared with the passive method alone. Han and Das [20] combined ultrasound with microneedles to enhance the permeability of the skin. He used bovine serum albumin (BSA) as a model of large molecules. Ultrasound and a 1.5 mm microneedles patch were used, which increased permeability of skin 10 times more than conventional methods. Table 1 presents the different drugs permeated into the skin by sonophoresis.

Many researchers have developed models to measure skin permeability. Johnson [21] developed a mathematical model to describe permeation via interkeratinocyte lipid domains. He further described that permeation through the skin depends on the transport properties of a microscale lipid bilayer, as well as the structure and dimension of the epidermis. Based on his model, Mitragotri [22] proposed four pathways of drug diffusion through the skin as follows: (i) free-volume diffusion through lipid bilayers; (ii) lateral diffusion along lipid bilayers; (iii) diffusion through pores; and (iv) diffusion through shunts. His research concluded that among the four pathways of permeation, transport through pores plays a vital role in hydrophilic solutes. Tezel [23] in his research discussed three modes of interaction that can increase skin permeability for macromolecules. Among these, cavitation plays the greatest role in enhancing the transdermal transport of molecules.

Many researchers have also worked on simulating the setup of transdermal delivery. Kwon et al. [24] modeled skin with a topical adsorptive layer in COMSOL Multiphysics software. They introduced impurities in the dermis that were aimed to be removed by the application of charcoal. Mass transport and charcoal were modeled by the transient diffusion equation and pseudo-first-order reaction kinetics, respectively. Kermani [25] used COMSOL Multiphysics simulation software to deliver fentanyl drug mixed with chemical enhancer lauryl, transdermally, using the diffusion equation. They simulated the model of skin and patch. The thickness of skin in this model was considered 50.8 µm, and it was assumed that drug and enhancer are uniformly dissolved in the patch. This simulation showed that after one hour of applying the patch, the concentration of the drug in the patch decreased. The drug was better penetrated when used with an enhancer.

Yuta Kurashina et al. developed a low-frequency piezoelectric Langevin transducer. The authors experimented with the transdermal penetration of silica, polystyrene, and gold nanoparticles into the skin. It is found that the penetration of these particles depends on the material and size, as well as the hardness of the subcutaneous support material [26]. A.S. Fiorillo et al. developed a piezopolymer device that works on a frequency of 20 kHz and the acoustic pressure (compressional and rarefactional) obtained on that frequency was equal to 2 kPa. Moreover, they concluded that this acoustic pressure can modify biological tissue when the distance of the ultrasound source is varied [27].

Lipeng He et al. in a study presented the relationship between flow rate from a piezoelectric pump and sound pressure level. The authors experimented with the change

in flow rate by changing the chamber depth of the piezoelectric pump. It has been observed that sound pressure level increases as voltage and frequency increase. As result, the highest sound pressure level achieved was 69 dB at 225 V with 1.5 mm of chamber depth. Sound pressure level versus frequency results showed that the highest sound pressure level was 76 dB at 320 Hz with a chamber height of 0.5 mm [28].

Table 1. Research on sonophoresis in transdermal drug delivery.

Drug	Molecular Weight of Drug in Daltons	Chemical Formula of Drug	Frequency	Sonication Time	Reference
Butanol	74	$C_4H_{10}O$	20 kHz	10%	[29]
Caffeine	194	$C_8H_{10}N_4O_2$	20 kHz	10 min, 1 h	[30]
Histamine	184	$C_5H_9N_3$	36 kHz	5 min	[31]
Ketoprofen	254	$C_{16}H_{14}O_3$	20 kHz	0.5–2 min	[32]
Bovine serum albumin	66,000	$C_{123}H_{193}N_{35}O_{37}$	20 kHz	2 min	[33]
Insulin	5807	$C_{257}H_{383}N_{65}O_{77}S_6$	20 kHz	60 min	[34]

3. Structure Design of Single-Element Piezoelectric Transducer

This section presents the fabrication procedure used to build the single-element piezoelectric transducer. Figure 1 shows the design of a piezoelectric transducer placed on the skin, using four blocks with dimensions given in Table 1. Block one is a backing layer of tungsten material, block two is a piezoelectric ceramic using PZT-5H, block three is a matching layer of aluminum, and block four is a model of the epidermis, i.e., the top layer of the human skin, where we intend to estimate acoustic pressure and SPL. Table 2 presents the dimensions used for the piezoelectric transducer and skin. The piezoelectric transducer is placed on the top of the skin membrane, which is 0.5 mm thick and has a length and width of 4 mm. The material parameter values of each block are given in Table 3. Table 4 presents the skin specifications given in COMSOL. These four blocks are placed on top of each other, and the function of each of these is defined by a module of COMSOL Multiphysics, as shown in Table 5.

Table 2. Dimensions used for piezoelectric transducer.

Parameter	Symbol	Material	Typical Value (mm)
PZT Thickness	t_p	PZT-5H	0.8
PZT Width and Height	w_p, h_p	-	0.8^2
Matching Layer Thickness	t_m	Alumina	2
Matching Layer Width and Height	w_m, h_m	-	2^2
Backing Layer Thickness	t_b	Tungsten	2
Backing Layer Width and Height	w_b, h_b	-	2^2
Boundary Interface Thickness	t_s	Skin	0.5
Boundary Interface Width and Height	w_s, h_s	-	4^2

Table 3. Material parameter values in FEM model.

Material	Density kg/m^3	Sound Velocity m/s
PZT-5H	7500	4319
Alumina	3960	9900
Tungsten	19,250	5200
Skin	1100	1540

Table 4. Built-in skin specifications in COMSOL.

Property	Variable	Value	Unit
Density	ρ	1109	kg/m^3
Heat capacity at constant pressure	C_p	3391	J/kg·K
Frequency factor	A	4.575×10^{72}	1/s
Activation energy	dE	4.71×10^5	J/mol
Young's modulus	E	1	Pa
Poisson's ratio	ν	1	1

Table 5. Modules used in simulation.

S. No.	Block	Multiphysics Module
1	Backing Layer	Solid Mechanics
2	Matching Layer	
3	Piezoelectric Ceramic	Electrostatics
4	Skin	Pressure Acoustics

4. Simulation of Piezoelectric Transducer Using COMSOL Multiphysics

To simulate the effect of the piezoelectric transducer on the skin, it is necessary to integrate all the blocks into a systemic whole. This is conducted by coupling the solid mechanics module with electrostatics and pressure acoustics modules.

In COMSOL Multiphysics, solid mechanics are found under the branch of Structural Mechanics. They are used to measure the effect of stress, strain, and displacement on the selected material. Meanwhile, the electrostatics module found under the AC/DC branch is used to compute the electric displacement field, electric field, and potential distributions in dielectric materials. The final module used in this simulation is pressure acoustics, frequency domain (acpr) found under the branch of pressure acoustics. It is used to compute the pressure variations caused by the propagation of acoustic waves in a selected medium. Here, backing and matching layers are selected as a domain in solid mechanics. Piezoelectric ceramic (PZT-5H) is selected within the electrostatics module. Skin membrane is selected as a domain for the measurement of acoustic pressure and SPL in acoustic pressure, frequency domain module. Coupling solid mechanics and pressure acoustics modules form an interface called the acoustic structure interaction boundary, which determines transfer effects between solid mechanics (stress, strain, or displacement) and pressure acoustics. The simulation is carried out for low frequencies used in sonophoresis (20–100 kHz) and voltages ranging from 1 mV to 10 mV.

4.1. Acoustic Pressure Calculation

The wave equation for sound is given as in Equation (1), which is used to find acoustic pressure variations p on the top of the stationary background pressure ${p_0}^4$

$$\frac{1}{\rho c^2}\frac{\partial^2 p}{\partial t^2} + \nabla.\left(-\frac{1}{\rho}(\nabla p - q_d)\right) = Q_m \tag{1}$$

Table 6 describes the symbols of Equation (1), which reduces to the following inhomogeneous Helmholtz equation in the frequency domain studies

$$\nabla.\left(-\frac{1}{\rho}(\nabla p - q_d)\right) - \frac{\omega^2 p}{\rho c^2} = Q_m \tag{2}$$

COMSOL uses finite element analysis [35] to solve Equation (2) for pressure (p).

Table 6. Description of symbols of wave equation.

Symbol	Description	Unit
ρ	Total density	kg/m^3
p	Pressure	Pa
p_b	Background pressure	Pa
c	Speed of sound	m/s
q_d	Dipole domain source	N/m^3
Q_m	Monopole domain source	rad^2/s^2
ω	Angular frequency ($2\pi f$)	rad/s

4.2. Sound Pressure Level

Sound pressure level is a logarithmic measure of the effective pressure of a sound relative to the reference value. It is measured in decibels. Equation (3) is copied from Ref. [36].

$$SPL = 20log\left(\frac{p_{rms}}{p_{ref}}\right) \quad (3)$$

where p_{rms} represents the root-mean-squared value of pressure p_{ref} = 1 µPas, which is the reference sound pressure for water. Considering the closeness of density and speed of sound in water and skin, we chose p_{ref} in skin, the same as in water.

5. The Simulation Results

We present two types of results. In the first case presented in Section 5.1, the frequency of the sinusoidal excitation is kept constant at 25 kHz, and the voltage varies from 1 mV to 10 mV. Meanwhile, in the second case presented in Section 5.2, the frequency varies from 20–100 kHz, while the peak voltage of the sinusoidal excitation is kept fixed at 1 mV. Hence, voltage and frequency are two factors that determine the SPL and acoustic pressure of a transducer with the specified characteristics.

5.1. SPL and Acoustic Pressure versus Voltage

Figure 2 shows the linear increase in acoustic pressure from 0.0072 Pascals to 0.72 Pascals, while the peak voltage grows from 1 mV to 10 mV. Figure 3 shows the SPL values calculated using Equation (3) from the response of Figure 2. The SPL grows from 94.1 dB to 114.1 dB for the one order of increase in the applied peak voltage.

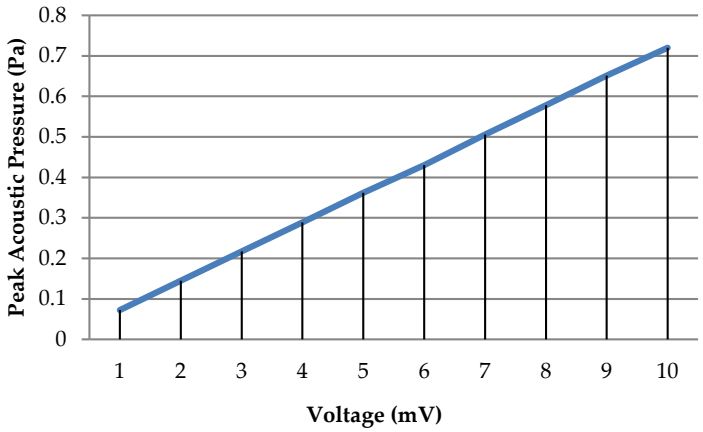

Figure 2. Total acoustic pressure versus voltage at 25 kHz.

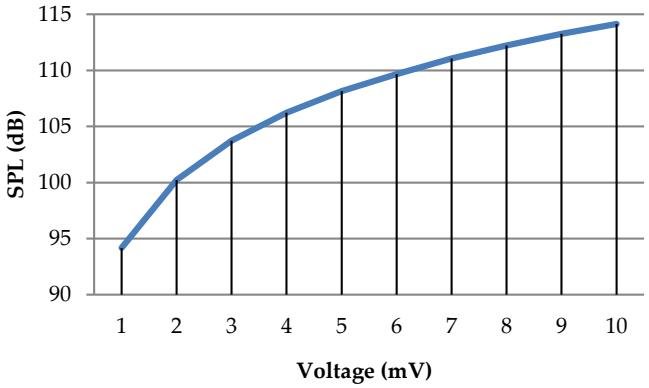

Figure 3. Sound pressure level versus voltage at 25 kHz.

5.2. Simulation of SPL and Acoustic Pressure versus Frequency

The results of the total acoustic pressure are depicted in Figure 4. One finds that the acoustic pressure exhibits exponential growth from 0.2 mPa to 5 mPa as the frequency increases from 20 kHz to 100 kHz. Meanwhile, in Figure 5, one finds that as the frequency varies from 20 kHz to 100 kHz, the SPL shows logarithmic growth from 43.01 to 70.96 dB. Figure 6 shows the frequency response of the transducer from 20 kHz to 1 MHz. The curve shows the irregular frequency response from 760 to 1000 kHz. Meanwhile, the highest peak of 186 dB occurs at the frequency of 880 kHz. It is observed from the literature review that the peak achieved at 880 kHz can be used in ophthalmology for delivering drugs.

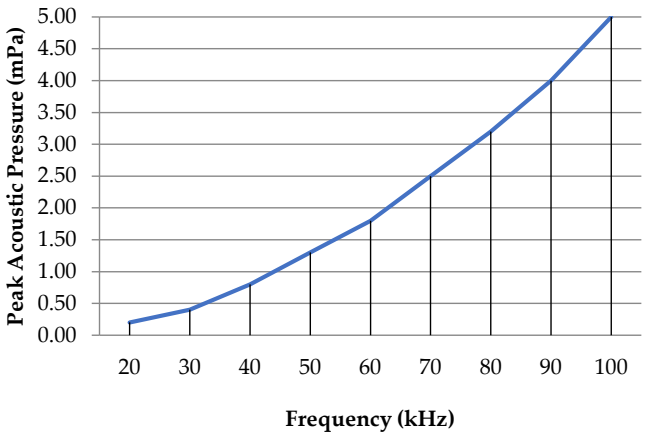

Figure 4. Total acoustic pressure versus frequency at 1 mV.

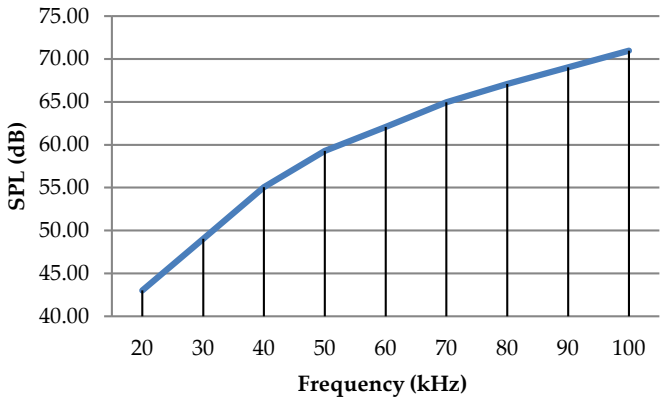

Figure 5. SPL versus frequency at 1 mV.

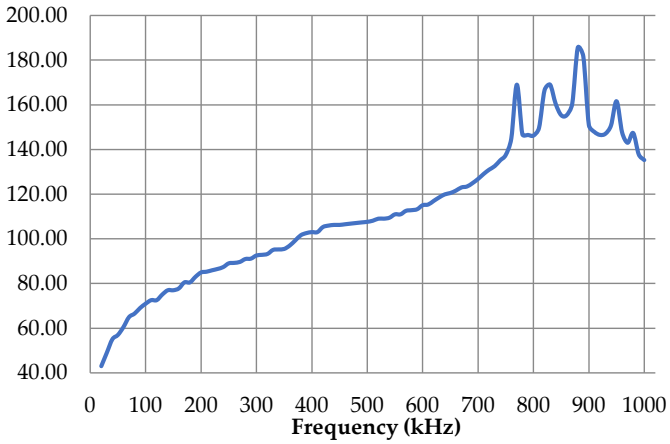

Figure 6. SPL versus frequency (20 kHz to 1 MHz) at 1 mV.

6. Conclusions

Drugs with a molecular weight greater than 500 daltons require a stimulus to move through the stratum corneum. Sonophoresis is one of the non-invasive active methods of stimulation. Hence, in this paper, a low-frequency sonophoretic piezoelectric transducer and human skin were simulated. The transducer was placed on simulated human skin to measure the acoustic pressure and SPL. The acoustic pressure and SPL were estimated for a range of peak driving voltages (1–10 mV) and frequencies (20–100 kHz). The acoustic pressure changes linearly with the applied peak voltage but varies exponentially with the frequency.

In future research work, we intend to introduce a drug-loaded patch placed between the matching layer and the skin membrane to study transdermal drug delivery using sonophoresis.

Author Contributions: Conceptualization, S.M., A.A.U. and A.M.; methodology, S.M. and A.A.U.; formal analysis, S.M. and A.A.U.; resources, Mendeley; writing—original draft preparation, S.M. and A.A.U.; writing—review and editing, B.S.C. and N.F.M.N.; supervision, A.A.U. and A.M.; project administration, B.S.C. All authors have read and agreed to the published version of the manuscript.

Funding: This research received no external funding.

Institutional Review Board Statement: Not applicable.

Informed Consent Statement: Not applicable.

Data Availability Statement: Not applicable.

Conflicts of Interest: The authors declare no conflict of interest.

References

1. Mitra, A.K.; Kwatra, D.; Vadlapudi, A.D. *Drug Delivery*; Jones & Bartlett Learning: Burlington, MA, USA, 2014.
2. Farhadieh, R.; Bulstrode, N.; Mehrara, B.J. *Plastic Surgery—Principles and Practice*; Elsevier: Amsterdam, The Netherlands, 2021; ISBN 9780323653817.
3. Park, D.; Song, G.; Jo, Y.; Won, J.; Son, T.; Cha, O.; Kim, J.; Jung, B.; Park, H.; Kim, C.W.; et al. Sonophoresis using ultrasound contrast agents: Dependence on concentration. *PLoS ONE* **2016**, *11*, e0157707. [CrossRef] [PubMed]
4. Jain, K.K. An Overview of Drug Delivery Systems. *Methods Mol. Biol.* **2020**, *2059*, 1–54. [CrossRef] [PubMed]
5. Li, C.; Wang, J.; Wang, Y.; Gao, H.; Wei, G.; Huang, Y.; Yu, H.; Gan, Y.; Wang, Y.; Mei, L.; et al. Recent progress in drug delivery. *Acta Pharm. Sin. B* **2019**, *9*, 1145–1162. [CrossRef] [PubMed]
6. Oberli, M.A.; Schoellhammer, C.M.; Langer, R.; Blankschtein, D. Ultrasound-enhanced transdermal delivery: Recent advances and future challenges. *Ther. Deliv.* **2014**, *5*, 843–857. [CrossRef] [PubMed]
7. Ita, K. Recent progress in transdermal sonophoresis. *Pharm. Dev. Technol.* **2017**, *22*, 458–466. [CrossRef]

8. Marwah, H.; Garg, T.; Goyal, A.K.; Rath, G. Permeation enhancer strategies in transdermal drug delivery. *Drug Deliv.* **2016**, *23*, 564–578. [CrossRef]
9. Mohammad, E.A.; Elshemey, W.M.; Elsayed, A.A.; Abd-Elghany, A.A. Electroporation parameters for successful transdermal delivery of insulin. *Am. J. Ther.* **2016**, *23*, e1560–e1567. [CrossRef]
10. Sá, G.F.F.; Serpa, C.; Arnaut, L.G. Stratum corneum permeabilization with photoacoustic waves generated by piezophotonic materials. *J. Control. Release* **2013**, *167*, 290–300. [CrossRef]
11. Park, J.; Lee, H.; Lim, G.-S.S.; Kim, N.; Kim, D.; Kim, Y.-C.C. Enhanced Transdermal Drug Delivery by Sonophoresis and Simultaneous Application of Sonophoresis and Iontophoresis. *AAPS PharmSciTech* **2019**, *20*, 96. [CrossRef]
12. Zhu, P.; Peng, H.; Mao, L.; Tian, J. Piezoelectric Single Crystal Ultrasonic Transducer for Endoscopic Drug Release in Gastric Mucosa. *IEEE Trans. Ultrason. Ferroelectr. Freq. Control* **2021**, *68*, 952–960. [CrossRef]
13. Zhou, Z.; Fan, W.; Lang, M.; Wang, Y. Transdermal bFGF delivery using low-frequency sonophoresis: An innovative potential therapy for osteoradionecrosis of jaws. *J. Med. Hypotheses Ideas* **2015**, *9*, 9–12. [CrossRef]
14. Schafer, M.E. Basic Science of Ultrasound in Body Contouring. In *Ultrasound-Assist. Liposuction*; Garcia, O., Jr., Ed.; Springer: Cham, Switzerland, 2020; pp. 9–21. [CrossRef]
15. Murphy, C.A.; Houghton, P.; Brandys, T.; Rose, G.; Bryant, D. The effect of 22.5 kHz low-frequency contact ultrasound debridement (LFCUD) on lower extremity wound healing for a vascular surgery population: A randomised controlled trial. *Int. Wound J.* **2018**, *15*, 460–472. [CrossRef]
16. Nguyen, H.X.; Banga, A.K. Electrically and Ultrasonically Enhanced Transdermal Delivery of Methotrexate. *Pharmaceutics* **2018**, *10*, 117. [CrossRef]
17. Mishra, S.; Unnikrishnan, L.; Nayak, S.K.; Mohanty, S. Advances in Piezoelectric Polymer Composites for Energy Harvesting Applications: A Systematic Review. *Macromol. Mater. Eng.* **2019**, *304*, 1800463. [CrossRef]
18. Chaulagain, B.; Jain, A.; Tiwari, A.; Verma, A.; Jain, S.K. *Passive Delivery of Protein Drugs through Transdermal Route*; Taylor and Francis Ltd.: Boca Raton, FL, USA, 2018; Volume 46, pp. 472–487.
19. Bashyal, S.; Lee, S. Delivery of biopharmaceuticals using combination of liposome and iontophoresis: A review. *J. Pharm. Investig.* **2015**, *45*, 611–624. [CrossRef]
20. Han, T.; Das, D.B. Permeability enhancement for transdermal delivery of large molecule using low-frequency sonophoresis combined with microneedles. *J. Pharm. Sci.* **2013**, *102*, 3614–3622. [CrossRef]
21. Johnson, M.E.; Blankschtein, D.; Langer, R. Evaluation of solute permeation through the stratum corneum: Lateral bilayer diffusion as the primary transport mechanism. *J. Pharm. Sci.* **1997**, *86*, 1162–1172. [CrossRef]
22. Mitragotri, S. Modeling skin permeability to hydrophilic and hydrophobic solutes based on four permeation pathways. *J. Control. Release* **2003**, *86*, 69–92. [CrossRef]
23. Tezel, A.; Mitragotri, S. Interactions of Inertial Cavitation Bubbles with Stratum Corneum Lipid Bilayers during Low-Frequency Sonophoresis. *Biophys. J.* **2003**, *85*, 3502–3512. [CrossRef]
24. Kwon, H.; Hess, M.; Polski, R.M. Simulation of Transdermal Toxin Expulsion via Adsorptive Dermal Patch Using COMSOL Multiphysics. In Proceedings of the 2013 COMSOL Conference, Boston, MA, USA, 9–11 October 2013.
25. Kermani, A. Transdermal Drug Delivery with Permeation Enhancer. In Proceedings of the 12th COMSOL Conference 2016 Boston, Boston, MA, USA, 5–7 October 2016.
26. Kurashina, Y.; Asano, R.; Matsui, M.; Nomoto, T.; Ando, K.; Nakamura, K.; Nishiyama, N.; Kitamoto, Y. Quantitative Analysis of Acoustic Pressure for Sonophoresis and Its Effect on Transdermal Penetration. *Ultrasound Med. Biol.* **2022**, *48*, 933–944. [CrossRef]
27. Fiorillo, A.S.; Grimaldi, D.; Pullano, S.A. Low frequency ultrasounds in medicine. In *Proceedings of the 2009 IEEE International Workshop on Medical Measurements and Applications, Cetraro, Italy, 29–30 May 2009*; IEEE: New York, NY, USA, 2009; pp. 212–214. [CrossRef]
28. He, L.; Wu, X.; Zhao, D.; Li, W.; Cheng, G.; Chen, S. Exploration on relationship between flow rate and sound pressure level of piezoelectric pump. *Microsyst. Technol.* **2020**, *26*, 609–616. [CrossRef]
29. Mitragotri, S.; Blankschtein, D.; Langer, R. Transdermal drug delivery using low-frequency sonophoresis. *Pharm. Res.* **1996**, *13*, 411–420. [CrossRef] [PubMed]
30. Boucaud, A.; Machet, L.; Arbeille, B.; Machet, M.C.; Sournac, M.; Mavon, A.; Patat, F.; Vaillant, L. In vitro study of low-frequency ultrasound-enhanced transdermal transport of fentanyl and caffeine across human and hairless rat skin. *Int. J. Pharm.* **2001**, *228*, 69–77. [CrossRef] [PubMed]
31. Maruani, A.; Vierron, E.; Machet, L.; Giraudeau, B.; Boucaud, A. Efficiency of low-frequency ultrasound sonophoresis in skin penetration of histamine: A randomized study in humans. *Int. J. Pharm.* **2010**, *385*, 37–41. [CrossRef] [PubMed]
32. Herwadkar, A.; Sachdeva, V.; Taylor, L.F.; Silver, H.; Banga, A.K. Low frequency sonophoresis mediated transdermal and intradermal delivery of ketoprofen. *Int. J. Pharm.* **2012**, *423*, 289–296. [CrossRef] [PubMed]
33. Dahlan, A.; Alpar, H.O.; Murdan, S. An investigation into the combination of low frequency ultrasound and liposomes on skin permeability. *Int. J. Pharm.* **2009**, *379*, 139–142. [CrossRef] [PubMed]
34. Al-Bataineh, O.; Lweesyb, K.; Fraiwanb, L. Noninvasive Transdermal Insulin Delivery Using Piston-Shaped PZT Transducers: In vivo Rabbits Evaluation. *Jordan J. Mech. Ind. Eng.* **2012**, *6*, 11–16.

35. Dechaumphai, P.; Dechaumphai, P.; Sucharitpwatskul, S. *Finite Element Analysis with COMSOL*; Alpha Science International, Limited: Oxford, UK, 2019.
36. Bai, X.; Geng, M.; Liu, S.; Tang, B.; Wang, L.; Wu, J. Research on ventilation and noise reduction of indoor substation based on COMSOL Multiphysics. In *Proceedings of the 2022 IEEE 5th International Electrical and Energy Conference (CIEEC), Nangjing, China, 27–29 May 2022*; IEEE: New York, NY, USA, 2009; pp. 3330–3335. [CrossRef]